Journal of Energy Research and Reviews

4(1): 50-69, 2020; Article no.JENRR.54074
ISSN: 2581-8368

Optimization of the Performance of Hybrid Solar Biomass Dryer for Drying Maize Using ANSYS Workbench

Jackis Aukah[1*], Mutuku Muvengei[2], Hiram Ndiritu[2] and Calvin Onyango[3]

[1]Engineering Division, Kenya Industrial Research and Development Institute, P.O.Box 30650, GPO, Nairobi, Kenya.
[2]Department of Mechanical Engineering, J.K.U.A.T. Main Campus Juja, Box 62000-00200, Nairobi, Kenya.
[3]Food Technology Division, Kenya Industrial Research and Development Institute, P.O.Box 30650, GPO, Nairobi, Kenya.

Authors' contributions

This work was done in collaboration among all the four authors. Author JA designed the study, performed the analysis and wrote the first draft of the manuscript. Authors MM, HN and CO supervised the study and analyzed the data. All the authors managed the literature search and wrote the final manuscript. All authors read and approved the final manuscript.

Article Information

DOI: 10.9734/JENRR/2020/v4i130119
Editor(s):
(1) Dr. Bojan Durin, Department of Civil Engineering, University of North, Varaždin, Croatia.
Reviewers:
(1) Chemutai Roseline, Bukalasa Agricultural College, Uganda.
(2) Marco Antonio Campos, Universidade Paulista, Brazil.
(3) Pankaj Balasaheb Gavali, Sanjay Ghodawat Institute, India.
(4) Dajsingchai Wongkhomton, Mahasarakham University, Thailand and Ramkhamhaeng University, Thailand.
Complete Peer review History: http://www.sdiarticle4.com/review-history/54074

Original Research Article

Received 19 November 2019
Accepted 26 January 2020
Published 03 February 2020

ABSTRACT

In this paper ANSYS workbench was used to optimize the performance of hybrid solar biomass dryer for drying shelled maize in order to find the optimal operating input variables when the air temperature within the drying chamber set within the permissible range at reasonably high flow velocity. Hybrid Solar dryer with biomass as a source of fuel for auxiliary heating during absence or low solar insolation is a feasible option for small scale maize farmers [1]. At times high temperatures are induced in this dryer which may result in grain fissures and breakage during milling, thus reducing the grain quality. Optimization results indicate that in order to keep the air

**Corresponding author: E-mail: aukajakiz@gmail.com;*

temperature within drying chamber to permissible range [2], the air velocity at collector inlet and biomass heat exchanger outlet should be improved to 3 m/s and 2.8 m/s respectively while the capacity of the biomass heat exchanger should also be enhanced to provide hot air at 85°C. It be concluded from the study that HSBD is suitable for drying maize as well as other agricultural products since continuous interrupted drying can be achieved. The capability of the dryer to maintain uniform temperature and air flow within the drying chamber enable high quality dried products within a short duration.

Keywords: Optimization; shelled maize; hybrid solar biomass dryer; ANSYS design exploration; simulation.

ABBREVIATIONS

CFD : Computational Fluid Dynamics
GI : Galvanized Iron sheet
HSBD : Hybrid Solar Biomass Dryer
UV : Ultra Violet
KIRDI : Kenya Industrial Research and Development Institute
DOE : Design of Experiments

SYMBOLS

k : *Turbulence kinetic energy per unit mass [m^2/s^2]*
ε : *Turbulence dissipation rate [m^2/s^3]*
t : *Time [s]*
T : *Temperature [K]*
u : *Velocity [m/s]*
λ : *Thermal conductivity [W/mK]*
μ : *Dynamic viscosity [kg/m/s]*
ρ : *Mass density [kg/m^3]*
R_e : *Reynolds number*
L : *Characteristic length [m]*

1. INTRODUCTION

Maize is the most important staple food for the majority of Kenyan population and it is usually harvested at high moisture content that needs to be reduced to recommended value to prevent mould growth as well as other microbial attacks so that it can be stored for a long time [3]. In addition proper drying of maize can minimize post-harvest losses and quality deterioration in terms of nutritional value, flavour, texture and aflatoxins contamination hence preserving of maize available for consumption and sale. In Kenya, drying of maize is accomplished mainly through open-sun drying or mechanized dryers, with limited application of solar dryers. Open-sun drying is the oldest, most inexpensive and extensively used option by majority of Kenyans especially in rural areas where 98% of the households grow maize [4]. This method though less expensive but is labour intensive, unreliable, time consuming, leads to non-uniform drying, requires considerably large drying fields and too unhygienic making grains more susceptible to deterioration due to pest infestation and fungal contamination [5].

Some medium and large scale farmers employ the use of mechanical conventional dryers which are very faster and give a better quality product, but are expensive and require significant amount of energy, resulting to high operational cost for drying [5]. Hence, the application of solar dryers seems to address open sun-drying disadvantages, though it has not been adopted by majority of Kenyan [5]. This method is eco-friendly and viable to small and medium scale farmers [5]. One of the substantial drawbacks of solar dryers is the dependency on weather and can only operate well during the day when there is adequate solar insolation [5]. Since maize is hygroscopic just like other grains, it should be dried continuously to a desired moisture content in order to prevent moisture re-absorption and internal cracks which develop as a result of thermal stresses arising from alternate heating and cooling.

Solar hybrid dryer incorporated with biomass stove heat exchanger system as an auxiliary heating source to complement solar energy during low insolation is a feasible option especially for small scale farmers [1]. Maize farmers suffer from high drying cost due to high energy demand and also inhomogeneous drying due to low air flow rate within the drying chamber [1]. At times high temperatures are induced in the dryer which may result in grain fissures and breakage during milling, thus reducing the grain quality. Local saturation of the drying air may also occur in the drying chamber before the desired moisture content of the maize is attained and this may result to condensation in the drying chamber.

Therefore there is a need to model and optimize the drying chamber and the drying process of the HSBD by predicting the air flow distribution, temperature profile and relative humidity in the dryer in order to improve its overall performance in drying of maize at minimum cost.

Optimization is a process of choosing the optimal input parameters so as to achieve the desired performance of the system in an automated manner, this is evaluated by means of output parameters. There are several choices to examine the system performance using a certain output parameter such as maximize its value, minimize its value, or seeking target value.

Solar drying systems must be properly designed to meet particular drying requirements of specific products and to give satisfactory performance with respect to requirements.

To attain good quality dried maize, the air temperature in the drying chamber should be within the permissible range. Performance optimization procedure was therefore conducted to find the optimal operating input variables when the air temperature within the drying chamber was set within permissible range at high flow velocity. Mutai et al. [5] considered 50°C as the permissible air temperature for drying maize while Prakash and Kumar [6] noted that the maximum drying temperature for maize grain is 60°C, therefore this is what was considered as the permissible range for optimization.

2. MATERIALS AND METHODS

Simulation was performed using ANSYS CFX in three dimensions in order to present factual and elaborate airflow inside the dryer [1]. Design exploration algorithm within ANSYS Workbench was used for optimization process, this was done by considering the permissible temperature for drying maize given by different researchers as the objective function. The dryer was simulated without considering the trays and products to be dried [1].

2.1 Description of Hybrid Solar Biomass Dryer

The main components of the developed HSBD are; solar collector, drying chamber and biomass stove heat exchanger system all constructed and assembled as one single unit as shown in Fig. 1 [1].

The main components of the dryer was designed to be assembled and disassembled with ease especially when relocating from one place to another, the dryer is fitted with lockable caster wheels for ease of mobility. The roof of the dryer was made in triangular shape and covered with UV treated plastic sheet. The absorber plate was painted black to easily absorb solar radiation,

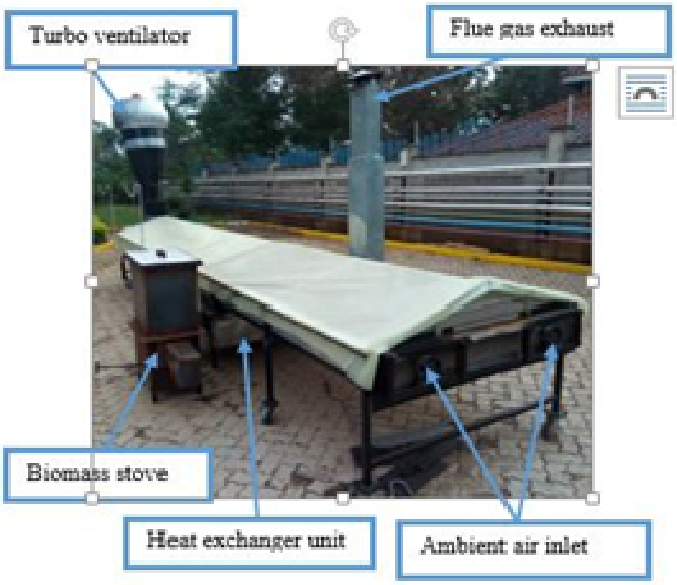

Fig. 1. Picture of assembled HSBD

convert it into heat energy and then releases it to heat the surrounding air. The main structural frame of the dryer was constructed using mild steel square hollow section and angle iron with the bottom part made of wooden material to act as insulation. The internal part of the dryer including the bottom/ floor were covered with alluminium painted galvanized sheet to reflect energy incident on it. The design capacity of the dryer is 90 kg (Wet basis) of maize per batch. The drying chamber has six removable drying trays made of galvanized mesh a lined with plastic mesh and then fitted to alluminium angle line frame as shown in Fig. 2 [2], The dimensions of the tray are 1 m by 0.6 m and are fixed horizontally at about 150 mm above absorber plate to permit smooth flow of drying air on top and beneath the product, hence eliminate the need of turning the product during drying as shown in Fig. 3. The dryer was designed to allow for loading and unloading of the product by lifting up the UV treated sheet cover as in Fig. 4 [3].

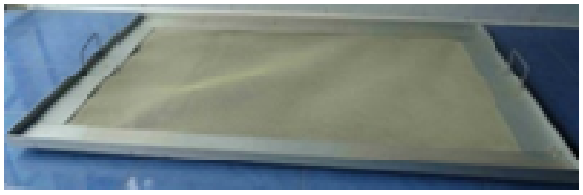

Fig. 2. Tray details

Fig. 3. Drying trays arrangement in HSBD

Fig. 4. Loading and unloading of products in HSBD

A biomass stove heat exchanger system was incorporated to the solar dryer to reduce its dependency on solar radiation by providing hot air to the drying chamber during low solar insolation or when the dryer is operated beyond sunshine hours, thus making it a hybrid dryer. The heat exchanger used was a cross flow type with flue gas from the stove passing through a duct with eight fins to enhance heat transfer between the flue gas and the air and then exits through the chimney located on the opposite side of the drying chamber. The air inlet to the heat exchanger is located at the bottom part of the shell to allow drying air to meet the flue gas duct at 90°. Wind cyclone was also fitted at the end of the drying chamber to facilitate the airflow within the dryer. The wind cyclone stack was painted black to improve the temperature of the air flowing through it to avoid condensation as the air exits the dryer [5]. The heat exchanger was designed to heat air to a temperature of 70°C which is slightly above the maximum permissible drying temperature for grains. A rectangular duct made of galvanized sheet and fitted with eight equi-spaced fins at the top and bottom to provide the required heat transfer area for the heat exchanger.

The duct was placed inside mild steel shell of length 1.22 m, width: 0.6 m and height: 0.16 m. Collector side was provided with three sliding doors which can be adjusted to regulate the amount of air entering the dryer. The doors were fitted with wire mesh to prevent insects and flies from entering the dryer [7].

2.2 Simulation and Optimization of HSBD

Optimization was conducted using ANSYS which is a commercial CFD software [1]. First simulation of the flow within the HSBD was performed using ANSYS CFX which is one of the most widely used commercial codes for engineering fluid flow due to its accuracy, robustness and convenience [8]. Design Exploration algorithm within the ANSYS Workbench was then used to obtain the optimal drying air temperature and velocity within the HSBD for drying maize. Optimization procedure used is shown in Fig. 5.

2.3 Simulation Procedure

2.3.1 Geometry creation

The geometry of the HSBD was developed using pro engineer modelling software with the dimensions taken from experimental setup and then exported to ANSYS Design Modeler which is specifically designed for the creation and preparation of geometry for simulation. The geometry of the HSBD was divided into two regions i.e. flow in the drying chamber and that in the collector area to enable analysis of each region to be carried out independently as shown in Fig. 6. Each region was considered as a fluid domain and then interfaced together using an option of domain interface during simulation. The complete model was then exported to the ANSYS ICEM for mesh generation [1].

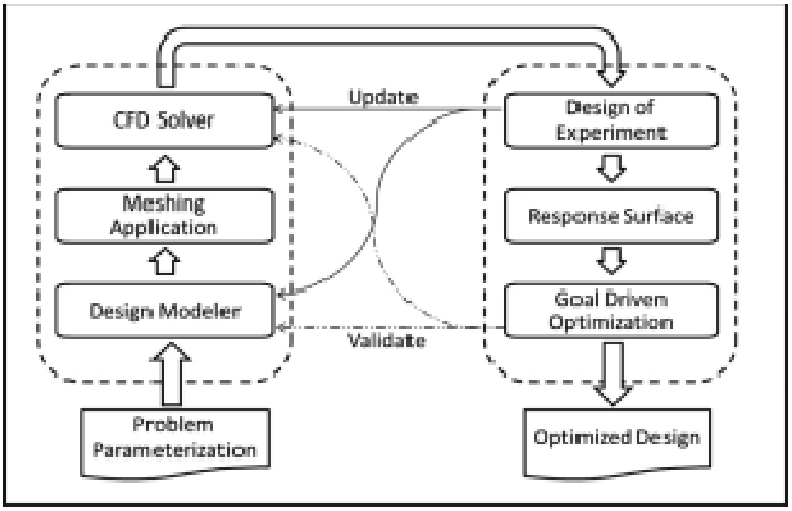

Fig. 5. Optimization flow chart

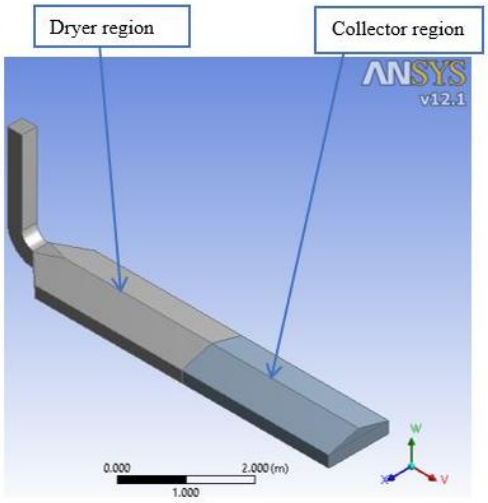

Fig. 6. 3D geometry of HSBD

2.3.2 Mesh generation

Mesh or grid development was done in ANSYS ICEM. In order to capture both the thermal and velocity boundary layers the entire model was discretized using three- dimensional unstructured hexahedral mesh elements which are accurate and involve less computation effort as indicated in Fig. 7. The mesh density was increased in the region around the wall edges and in the outlet air ducts (turbo ventilator stalk) where large gradients exist. The mesh size was decided after carrying out a preliminary grid independency analysis with different mesh resolutions to ensure that the numerical results were independent of the mesh density. The mesh in the regions near walls, edges and at the turbo ventilator stack were refined [1].

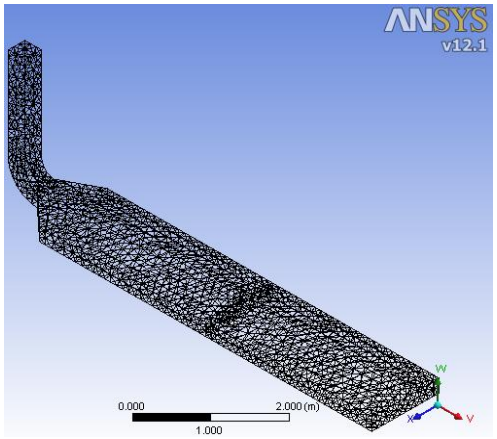

Fig. 7. Mesh from the geometry on ANSYS ICEM CFD

2.3.3 Simulation set up

The numerical simulation of flow inside the HSBD was done on basis of following basic assumptions:

- Problem is considered 3D and steady state
- Constant fluid properties
- Flow is assumed to be turbulent
- Ambient temperature is considered constant
- Incompressible fluid flow
- The walls were assumed to be smooth hence any disturbances in flow due to roughness of the surface were neglected.

The simulation was done at steady state condition and the physical time scale setting was used in order to achieve this condition. Physical Timescale provide sufficient relaxation of the equation non-linearity so that a converged steady state solution is obtained. The properties of the two domains were assumed to be the same and are as specified in Table 1. Both domains were connected using general connection interface between fluid and fluid domain without any wall. The working fluid was assumed to be an Ideal gas at 25°C with reference pressure of 1 atm. The characteristics of the working fluid are shown in Table 2 [1]. The flow characteristics inside the HSBD were predicted by calculating the Reynolds number using the following equation:

$$R_e = \frac{\rho u L}{\mu}$$

Where: R_e , ρ , u, L and μ are Reynolds number, density of air at 70°C (Kg/m^3), Velocity (m/s), Characteristic length (m) and Dynamic viscosity (Kg/ms). Calculation predicted that the flow was turbulent since the Reynolds number was 582786. Therefore a $k-\varepsilon$ turbulence model was added in the simulation. The solver control parameters were specified in the form of solution scheme and convergence criteria. High resolution differencing scheme was selected for the simulation since it produces more accurate results compared to upwind and central difference scheme. Room Mean Square residual type was used as the convergence criteria with residual target of 1.0e^{-6} for mass and momentum equations and 1.0e^{-3} for energy conservation equation [1].

Table 1. Domain properties

Properties	Domains (Dryer and collector)
Domain type	Fluid
Domain motion	Stationary
Material	Air assumed as an ideal gas at 25°C
Buoyancy model	Non-buoyant
Pressure	Reference pressure 1[atm]
Heat transfer model	Thermal energy
Turbulence model	$k-\varepsilon$ model
Thermal radiation model	Monte-Carlo
Spectral model	Gray

Table 2. Air properties

Properties	Value
Molar mass	28.96 Kg/Kmol
Specific heat capacity	1004 J/KgK
Dynamic viscosity	1.83 x 1e $^{-05}$ Kg/ms
Thermal conductivity	0.0261 W/mK
Refractive index	1
Density	1.185 Kg/m^3
Absorption coefficient	0.01/m
Scattering coefficient	0

2.3.4 Boundary conditions

The numerical solution of governing conservation [9,10] involves the use of specific boundary conditions, in particular at surfaces bounding of the domain as shown in Fig. 8. The set-up of boundary conditions were defined as described in this section:

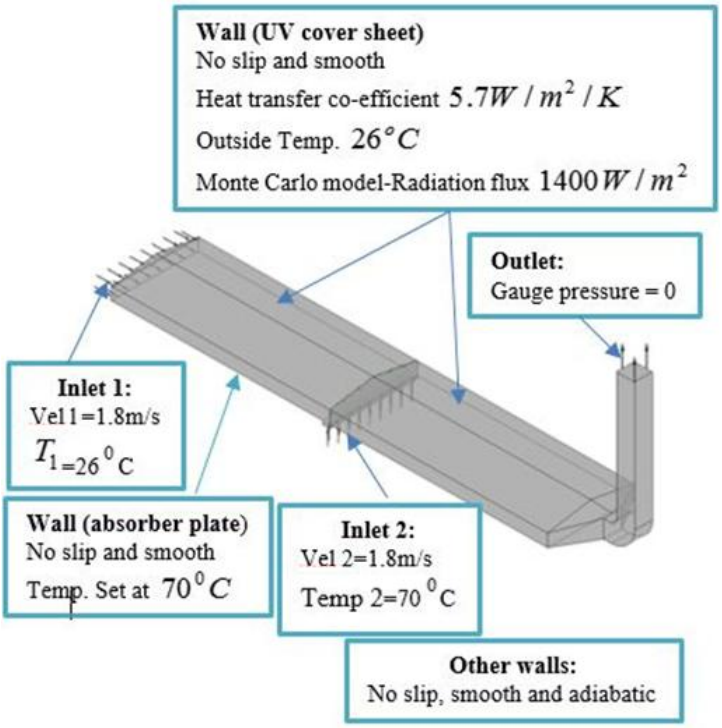

Fig. 8. Set up of boundary conditions

The first inlet was through the ambient air inlet indicated in Fig. 1 (collector chamber), the average velocity of 1.8 m/s obtained experimentally was used as the inlet velocity with a turbulent intensity of 5% (recommended if no information on inlet turbulence is available). The direction of flow was set normal to inlet while and air entering at ambient temperature of 26°C [1].

The second inlet is through the heat exchanger to the drying chamber, the average velocity of 1.8 m/s also obtained experimentally was used as the inlet velocity with a turbulent intensity of 5% (recommended if no information on inlet turbulence is available) [1]. The direction of flow was set normal to the inlet, and the biomass heat exchanger system was constructed to provide drying air at 70^0C to the drying chamber [1].

The dryer outlet was set to a gauge pressure of 0 Pa while the flow regimes at both inlet and outlet boundaries was specified as subsonic.

No slip and smooth wall boundary conditions were assumed at the walls since the velocity near the walls were set at zero equal to that of the wall (i.e. wall is stationary). The temperature at the walls was set out considering the measured experimental values and applying a boundary condition of Dirichlet type. At the UV sheet walls, heat transfer co-efficient of 5.7 W/m^2/K [11] and outside temperature of 26°C were used. Monte Carlo technique was used to model solar radiation with directional radiation flux of 1400 W/m^2. At absorber plate the temperature was set at 70°C and this value was from the experimental data [1]. The other walls were treated with the default boundary conditions of no slip, with smooth and adiabatic walls due to insulation. For the necessary turbulent quantities at boundaries, the CFX default boundary conditions for turbulence model were employed. The models constants were assumed as the default values considered in the CFX code.

2.4 Optimization Procedure

The optimization is a process of choosing the optimal input parameters so as to achieve the desired performance of the system in an automated manner, this is evaluated by means of output parameters. There are several choices to examine the system performance using a certain output parameter such as maximize its value, minimize its value, or seeking target value. Design Exploration algorithm within the ANSYS Workbench was used for optimization process.

Solar drying systems must be properly designed to meet particular drying requirements of specific products and to give satisfactory performance with respect to the requirements.

In order to achieve high quality dried maize, the air temperature in the drying chamber should be within the permissible range. Therefore to optimize the performance of the HSBD for drying maize, the following operating input variables were considered;

- Inlet air temperature and velocity from the biomass heat exchanger system (i.e. T_2=Temp 2 and V=Vel 2)
- Inlet air velocity from the solar collector side (i.e. u=Vel 1)

Performance optimization procedure was therefore conducted to find the optimal operating input variables when the air temperature within the drying chamber was set within permissible range at high flow velocity. Tonui et al. [5] considered 50°C as the permissible air temperature for drying maize while Garg and Prakash [12] noted that the maximum drying temperature for maize grain is 60°C, therefore this is what was considered as the permissible range for optimization. Since the drying air temperature distributed in the drying chamber was observed to be uniform [13], a point was chosen at the center on a plane within which drying trays are fitted and the air temperature set to permissible value of 50°C with the upper bound value set to maximum drying temperature of 60°C [1]. For the purpose of finding the set permissible value and maximum air velocity of the object function subjected to constraints as shown in Table 3, response surface optimization model was initiated and linked together with the CFX process as shown in Fig. 9.

The response surface optimization was done in three steps as shown in Fig. 10.

2.4.1 Design of experiments (DOE)

The first step for response surface optimization was to create design of experiments (DOE). In order to create a response surface, the value of the function was calculated at different combinations of the input parameters. DOE technique locates the sampling points in the design space by exploring the space for random input parameters in order to obtain the required information with minimum sampling points. Central composite design method was used to

select and create these design points based on the range given for the three input parameters to achieve optimized drying conditions for the HSBD to dry maize as in Table 4. The input parameter ranges shown in Table 4 was from experimental values ranging from minimum to maximum. The variation in the velocity was as a result of fluctuation of the ambient wind while that of temperature was due to heating value of the biomass material utilized as fuel to biomass stove [14]. Fifteen Design Points were randomly created and one of the points used to generate test sample after which the optimizer was updated to generate output (average temperature and velocity) values of the other points automatically. The design point generated depends on the number of input parameters [13].

Table 3. Objective and constraints of the optimization study

Table of Schematic B4: Optimization

	A	B	C	D	E	F	G
1	Name	Parameter	Objective		Constraint		
2			Type	Target	Type	Lower Bound	Upper Bound
3	Seek P7 = 323 K; P7 <= 333 K	P7 - Temp	Seek Target	323	Values <= Upper Bound		333
4	Maximize P6	P6 - Vel	Maximize		No Constraint		
*		Select a Parameter					

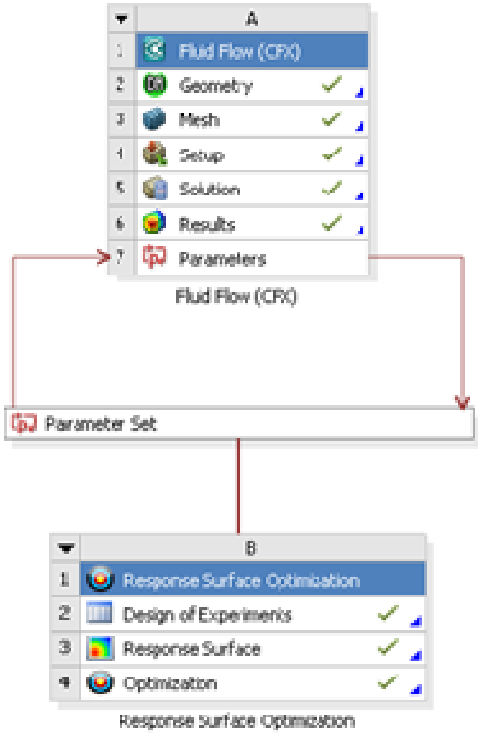

Fig. 9. ANSYS optimization entire workflow

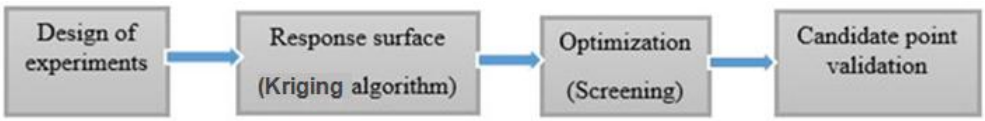

Fig. 10. ANSYS response surface optimization steps

Table 4. Input parameters and range

Input parameters	Minimum range	Maximum range
Velocity inlet 1 (m/s)	1.5	2
Air temperature inlet 2 (K)	309	378
Velocity inlet 2 (m/s)	1.5	2

2.4.2 Response surface

In this step, a Kriging Algorithm was employed to form a response surface from the generated values in the DOE table because of the ability of its internal error estimator to improve response surface quality by generating refinement points and adding them to the areas of the response surface that mostly require improvement, it also offers an auto refinement option which automatically and iteratively updates the refinement points during the update of the Response Surface [13]. The predicted response surface was used to get the value of the output variables to any combination of the input parameters without the need to perform a complete simulation.

2.4.3 Optimization

In this step a screening method was employed to obtain the optimal input parameters that achieved the desired performance of the HSBD using a comparative study by checking the output parameters seeking target value [13]. It uses the properties of the input as well the output parameters, and uses the Decision Support Process on a sample set generated by the Shifted Hamersley technique to rank and report the candidate designs of which the best is chosen. The best candidate point was chosen by considering the number of gold stars or red crosses displayed next to each goal-driven parameter which shows how well the parameter satisfies the stated goal with three red crosses indicating worst points while three gold stars indicate the best candidate point [13]. The maximum possible number of candidates to be generated and displayed by the algorithm was set at default, which is three, from which the best candidate was chosen. Since interpolation was used to find the response surfaces, it was important to validate the candidate points. This was done by calculating the exact values of the state functions and the optimization parameter at the candidate points and checking whether they fall within an acceptable range.

3. RESULTS AND DISCUSSION

As mentioned in section 2.4, the main goal of the study was to optimize the performance of the HSBD for drying maize by varying the input operating variables to obtain permissible drying air temperature at reasonably high velocity in the drying chamber.

3.1 Design of Experiments

Table 5 shows DOE with the generated output values from the created fifteen design points. It can be seen in Table 4 that the generated design points for the three input parameters (i.e. vel1, temp2 and vel2) are distributed between their minimum and maximum values. Column 5 and 6 of the table shows the estimated and predicted output parameter response data of any input parameters after performing the analysis.

3.2 Fitting the Response Surface

Fig. 11 represents results of variation of simulated temperature against actual temperature observed from the design points.

It can be observed from Fig. 11 that the points tend to lie along the diagonal line indicating that the simulated temperature of the drying chamber correctly fits the actual points of the design of experiments. Coefficient of determination presented a value of R^2 = 1 indicating that there was a good fit between the simulated and actual temperature of the design point [13].

Fig. 12 represents results of variation of simulated velocity against actual velocity observed from the design points.

It can be seen from 12 that the points tend to lie along the diagonal line indicating that the simulated velocity of the drying chamber correctly fits the actual points of the design of experiments. Coefficient of determination presented a value of R^2 = 1 indicating that there was a perfect agreement between the simulated and actual velocity of the design point [13].

3.3 Response Surfaces

Fig. 13 represents results of three dimensional contour response chart for the variation of temperature in the drying chamber (Temp) with respect to inlet velocity from collector side (Vel1)

and inlet air temperature from the biomass heat exchanger (Temp2). It displays a selected input on the X axis, a selected input on the Y axis, and a selected output on the Z axis.

Table 5. Design of experiments (Central composite design)

Name	P1-Vel1 (m/s)	P2-Temp2 (K)	P5-Vel2 (m/s)	P6-Vel (m/s)	P7-Temp (K)
1	1.75	343.5	1.75	2.2998	319.18
2	0.5	343.5	1.75	1.218	335.25
3	3	343.5	1.75	3.3162	313.15
4	1.75	309	1.75	2.3016	306.68
5	1.75	378	1.75	2.2971	330.04
6	1.75	343.5	0.5	1.7068	309.61
7	1.75	343.5	3	2.8139	326.87
8	0.73371	315.45	0.73371	0.98518	310.89
9	2.7663	315.45	0.73371	2.6418	305.17
10	0.73371	371.55	0.73371	0.98331	329.14
11	2.7663	371.55	0.73371	2.6339	311.1
12	0.73371	315.45	2.7663	1.8602	315.44
13	2.7663	315.45	2.7663	3.6041	308.54
14	0.73371	371.55	2.7663	1.8454	354.1
15	2.7663	371.55	2.7663	3.6006	327.75

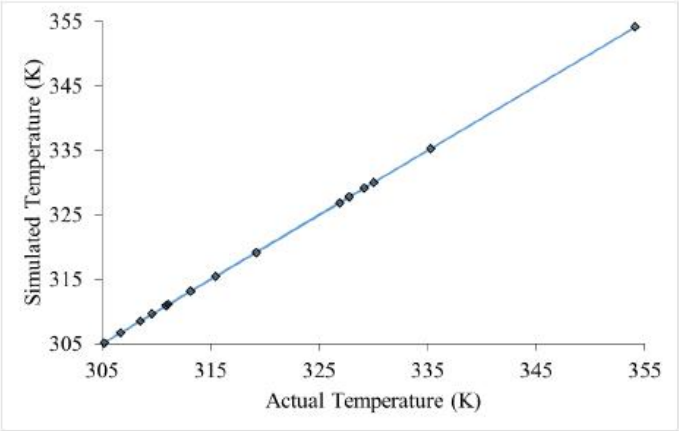

Fig. 11. Variation of simulated temperature against actual temperature

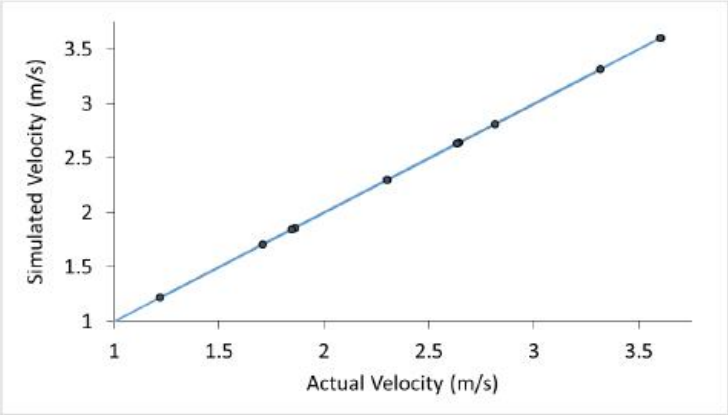

Fig. 12. Variation of simulated velocity against actual velocity

It can be noted from Fig. 13 that the air temperature in the drying chamber increases with the increases of air temperature from biomass heat exchanger but decreases as the air velocity from collector side is increased. Therefore, high air temperature within the drying chamber can be attained by keeping the air velocity at collector inlet low [1].

Fig. 14 represents results of three dimensional contour response chart for the variation of temperature in the drying chamber (Temp) with respect to inlet air velocity from collector side (Vel1) and inlet air velocity from the biomass heat exchanger (Vel2).

It can be noted from Fig. 14 that the air temperature in the drying chamber increases with the increases of air velocity from biomass heat exchanger but decreases as the air velocity from collector side is increased. This implies that air velocity from the collector inlet must be kept low in order to maintain high temperature in the drying chamber.

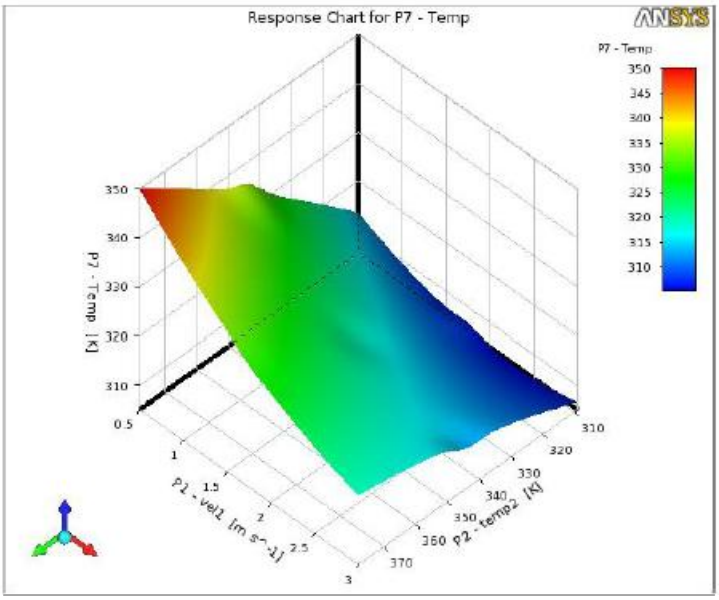

Fig. 13. Variation of temp versus Vel1 and Temp2

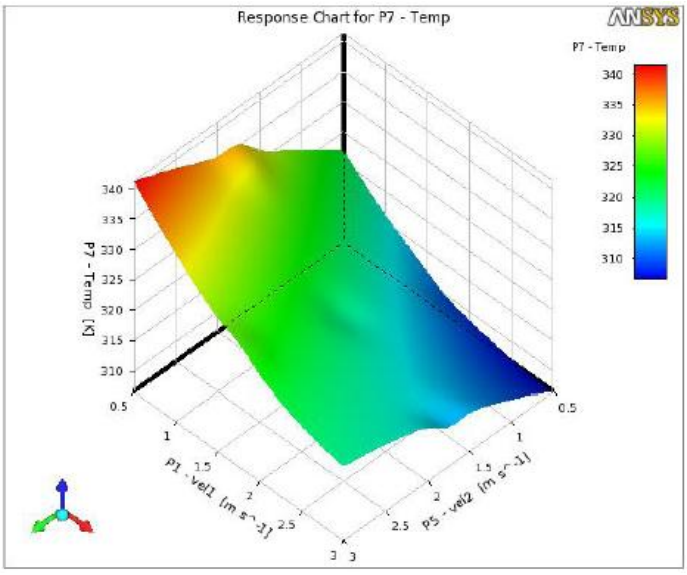

Fig. 14. Variation of temp with respect to Vel1 and Vel2

Fig. 15 represents results of three dimensional contour response chart for the variation of temperature in the drying chamber (Temp) with respect to inlet air temperature (temp2) and inlet air velocity from the biomass heat exchanger (Vel2).

From Fig. 15, it can be seen that air temperature in the drying chamber increases with the increases of both air velocity and air temperature from biomass heat exchanger. This implies that both air velocity and air temperature from the biomass heat exchanger must be kept high in order to maintain high temperature in the drying chamber.

Fig. 16 represents results of three dimensional contour response chart for the variation of drying air velocity within the drying chamber (Vel) with respect to air velocity from collector inlet (Vel1) and air temperature from biomass heat exchanger (Temp2) [1].

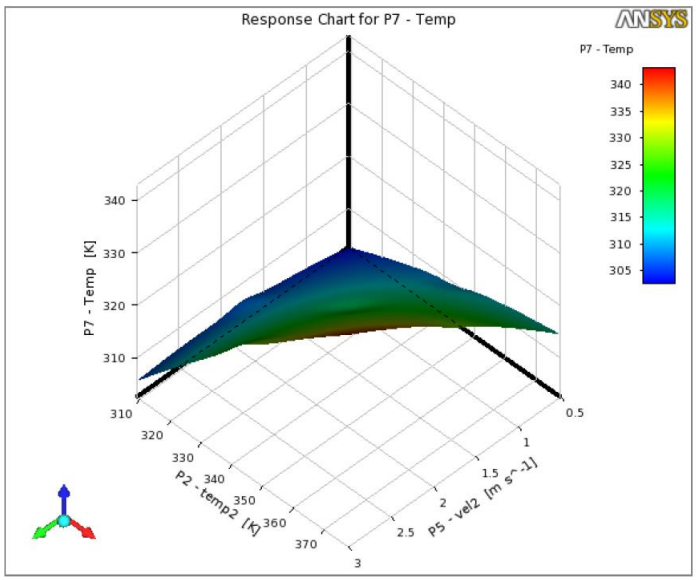

Fig. 15. Variation of temp versus Vel2 and Temp2

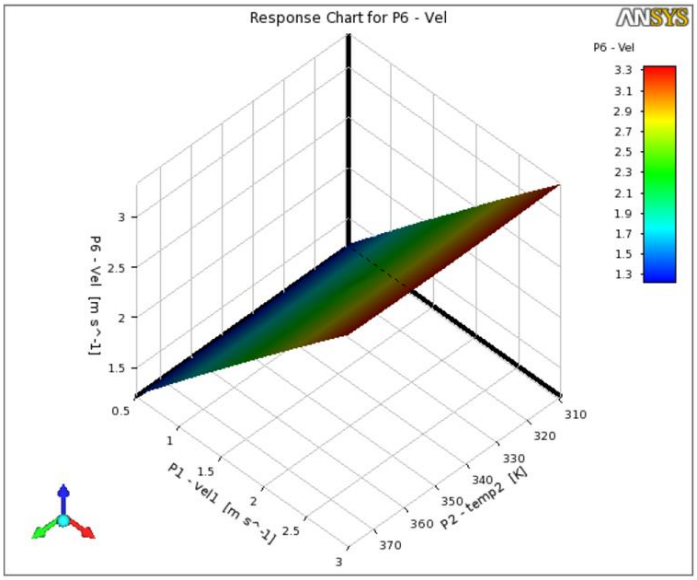

Fig. 16. Variation of Vel versus Vel1 and Temp2

From Fig. 16, it can be seen that drying air velocity within the drying chamber increases linearly with air velocities at collector inlet, but it is not affected by air temperature from heat exchanger [1]. This implies that high air velocity can be achieved by keeping the air velocity at collector inlet high.

Fig. 17 represents results of three dimensional contour response chart for the variation of drying air velocity within the drying chamber (Vel) with respect to air velocity from collector inlet (Vel1) and air velocity from biomass heat exchanger (Vel2) [1].

From Fig. 17, it can be seen that drying air velocity within the drying chamber varies linearly with air velocities at collector inlet and heat exchanger outlet and increases with the increase of the two input parameters [1]. This implies that when high velocity is required in the drying chamber then both the inlet air velocities from collector and biomass heat exchanger must be kept high.

Fig. 18 represents results of three dimensional contour response chart for the variation of drying air velocity within the drying chamber (Vel) with respect to air temperature Temp2) and air velocity from biomass heat exchanger (Vel2) [1].

From Fig. 18, it can be seen that drying air velocity within the drying chamber is influenced by air velocity from heat exchanger only [1]. This implies that when high velocity is required in the drying chamber then air velocity from the biomass heat exchanger must be kept high.

Since drying air temperature from the heat exchanger does not affect the drying air velocity within the drying chamber [5], it can be concluded from Figs. 13-18 that when high air velocity is required in the drying chamber then all the input velocities must be kept high.

Fig. 19 shows the results of local sensitivity of drying air velocity within the drying chamber to the input parameters (i.e. air velocity from collector inlet, air velocity and temperature from biomass heat exchanger) [1].

It is evident from Fig. 19 that drying air velocity within the drying chamber is mostly influenced by air velocity at the collector inlet since it provides the main airflow in the dryer, and moderately influenced by air velocity at the heat exchanger outlet while air temperature at the heat exchanger outlet has no effect on the drying chamber air velocity [1].

Fig. 20 shows the results of local sensitivity of air temperature in the drying chamber to the input parameters (i.e. air velocity from collector inlet, air velocity and temperature from biomass heat exchanger).

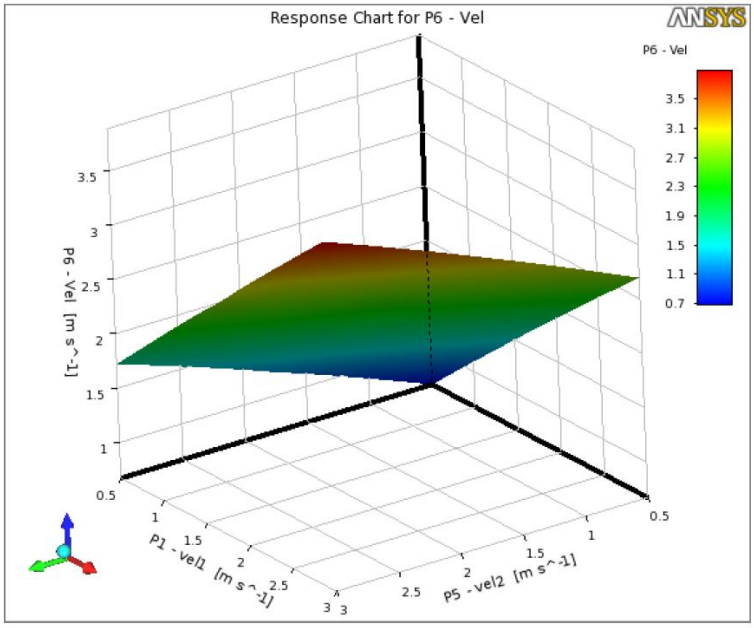

Fig. 17. Variation of Vel versus Vel2 and Vel1

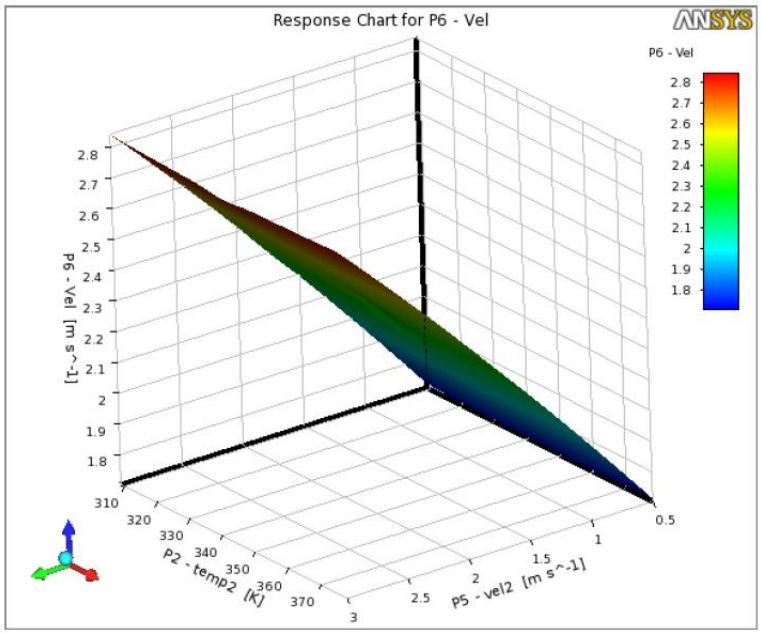

Fig. 18. Variation of Vel versus Vel2 and Temp2

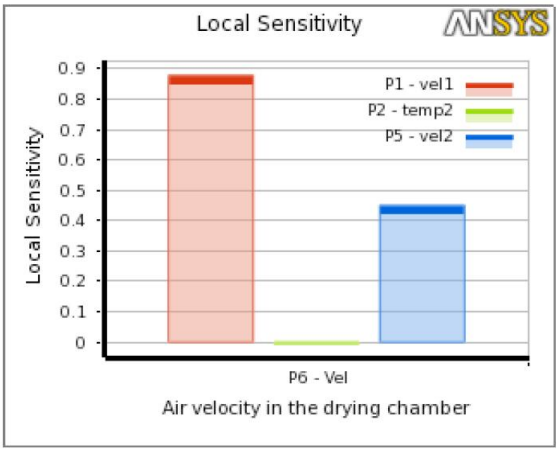

Fig. 19. Local sensitivity chart for variation of Vel against Vel1, Vel2 and Temp2

It can be observed from Fig. 19 that air temperature in the drying chamber is influenced by all the input parameters either positively or negatively. Any increase in air velocity and temperature at the heat exchanger outlet increases the air temperature in the drying chamber, while an increase of the air velocity at inlet reduced the air temperature in the drying chamber.

Therefore, it can be concluded from Figs. 19-20 that to improve the air temperature in the drying chamber without interfering with air velocity in the chamber, the air temperature of the biomass heat exchanger need to be increased. Increase in air velocity at the biomass heat exchanger outlet increases both drying air temperature and velocity within the drying chamber, so the air velocity at biomass heat exchanger should be kept high [5]. Any increases of the air velocity at collector inlet both increases air velocity and reduces air temperature in the drying chamber and this may require closer examination to find the right trade-off between the permissible drying air temperature and reasonable air velocity in the drying chamber.

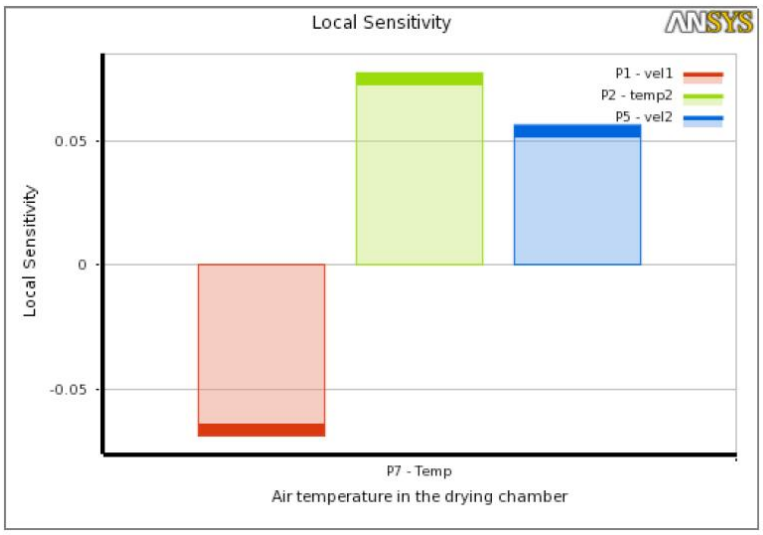

Fig. 20. Local sensitivity chart for variation of temp against Vel1, Vel2 and Temp2

3.4 Goal Driven Optimization

Table 6 shows the best 3 candidate points generated by screening optimization method as explained in section 2.4.3, each candidate point was displayed along with its input and output values. It can be seen from the Table 6 that both candidate point 1 and 2 present the best points since they display three gold star for both output target temperature and air velocity within the drying chamber. On the other hand, candidate point 3 present slightly higher output air velocity and a weaker output target temperature than candidate points 1 and 2. Therefore candidate point 1 is considered the best choice compared to the two since its output temperature value is much closer to the target value and also its output velocity value is kept sufficiently high. For best drying efficiency and maintaining grain quality, the air flow rate must be kept high to be able to carry away moisture from the product to exhaust port before it condenses within the dryer.

Candidate point 1 was then verified by creating and updating design points using the input parameter values. The deviation of the verified from unverified candidate point 1 was very small indicating that the response surface obtained is very accurate and require no refinement or adjustment. The verified candidate point 1 is placed below the row containing candidate point 1 as shown in Table 6.

Fig. 21 shows the tradeoff plot between drying air temperature and velocity within the drying chamber corresponding to the dominant Pareto fronts [5]. Dominant Pareto points are points when considered inferior in regard to other points and does not offer the best solutions for any optimization objective.

In Fig. 21 the design points represented by the red colour indicated the worst set of samples generated while the data points marked as blue blocks are considered as the best Pareto points

Table 6. Candidate points of the optimization study

	P1-Vel1 (m/s)	P2-Temp2 (K)	P5-Vel2 (m/s)	P7-Temp (K)	P6-Vel (m/s)
Candidate Point 1	2.9738	359.64	2.8206	323.83	3.7888
Candidate Point 1 (verified)	2.9738	359.64	2.8206	323.06	3.798
Candidate Point 2	2.8838	351.55	2.8069	321.56	3.7066
Candidate Point 3	2.9963	337	2.9132	316.4	3.8486

within the design space. The Pareto optimum points were picked out from the first sample set generated and then genetic algorithm was performed until a good set of likely points were generated [15].

The results of the best candidate points and their reference design points are shown in Table 6 [15].

Fig. 22 shows the tradeoff plot between air temperature and velocity in the drying chamber corresponding to the non-dominant Pareto fronts. Non-dominant Pareto points are points that offer best solutions for any optimization objective. These points are achieved by reducing slider in the properties view to reduce the fronts, consequently reducing the points. The points that are removed first are considered inferior and less adequate to the stated goal. It provides a choice of possible non-dominated solutions from which to choose from.

It can be seen from Fig. 22 that several points are located on the vertical line corresponding to drying air temperature of 323 K which was the main objective target.

3.5 Feasible Design

The values given for candidate point 1 considered to be the best amongst the three may not represent input parameter values that can be achieved. The values of the input parameters were then rounded off to a more acceptable values that realistically represent manufacturing capabilities by considering the influence each value has on the air velocity and temperature of the drying chamber based on the sensitivity curves. The rounded off input values provided better output values compared to the response surface provided by candidate point 1 as indicated in Table 7.

Full simulation of the model with the updated optimized input values was done to check the accuracy of the prediction. The air velocity and temperature in the drying chamber for un-optimized and optimized models were compared along the line shown in Fig. 23.

Fig. 24 shows comparison of air temperatures in drying chamber between the base and optimized model. It was observed from Fig. 24 that the air temperature was improved from 46°C to 50°C indicating that the air temperature in the drying chamber has been improved to attain permissible temperature for drying maize. There was a high temperature observed at a distance of 0.5 m from the heat exchanger inlet to the drying chamber as a result of hot air entering drying chamber from the biomass heat exchanger [1]. The temperature of air then came down after mixing with the air from the collector outlet and the mixture attaining a uniform value.

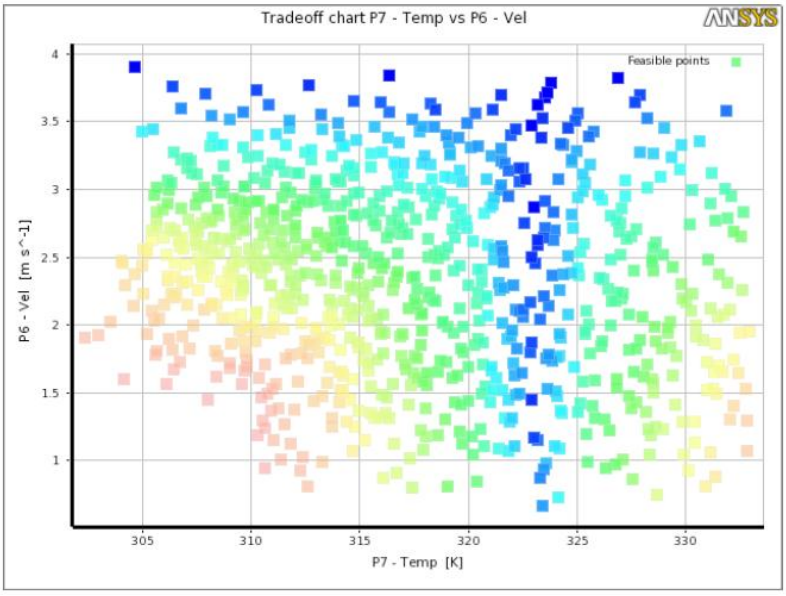

Fig. 21. Tradeoff plot between air temperature and velocity in the drying chamber for the dominant Pareto fronts

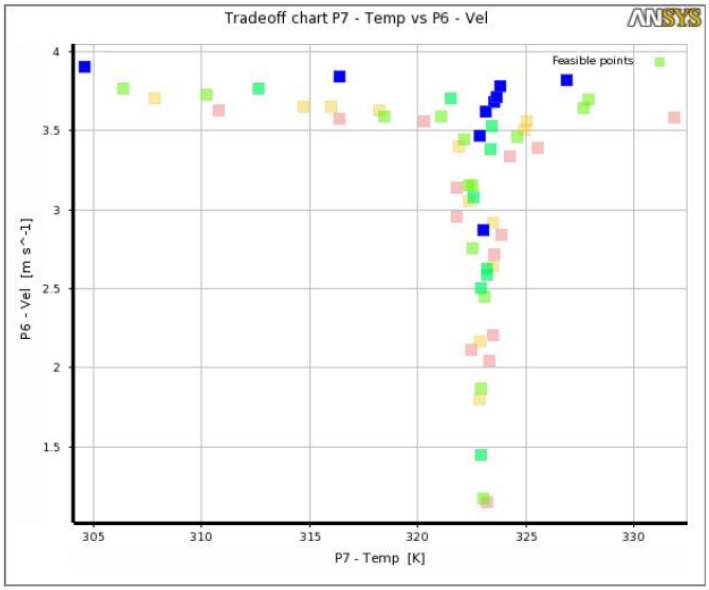

Fig. 22. Tradeoff plot between air temperature and velocity in the drying chamber for non-dominant Pareto fronts

Table 7. Rounded off input values

Name	P1-Vel1 (m/s)	P2-Temp2 (K)	P5-Vel2 (m/s)	P6-Vel (m/s)	P7-Temp (K)
Response Point	1.75	343.5	1.75	2.2998	319.18
Response Point 1 (candidate point 1)	2.9738	359.64	2.8206	3.7888	323.83
Response point 2 (rounded off Values)	3	358	2.8	3.8011	323.13

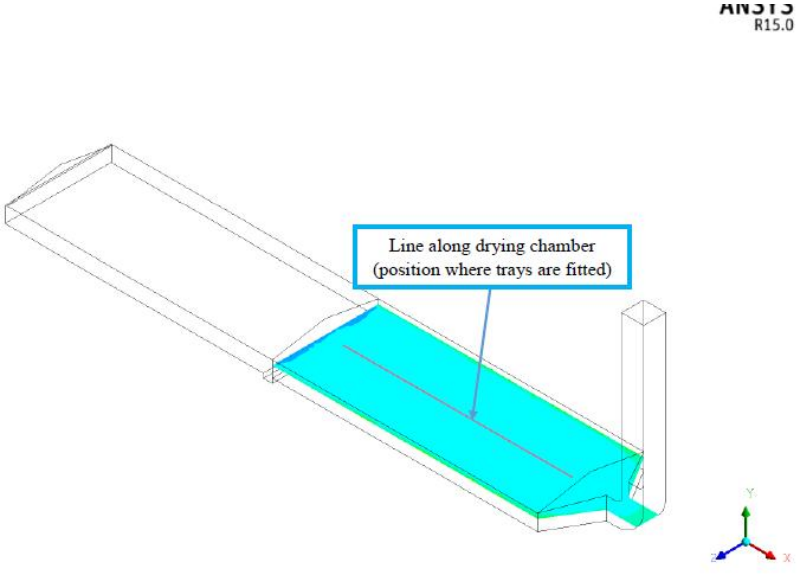

Fig. 23. Line along the drying chamber where air temperature and velocity were taken

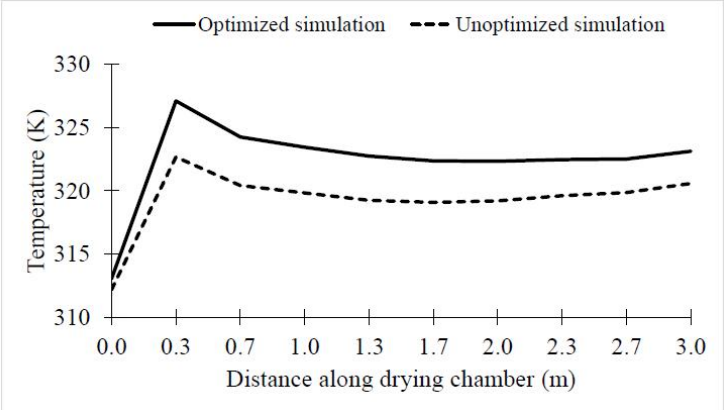

Fig. 24. Air temperature comparison before and after optimization along the drying chamber

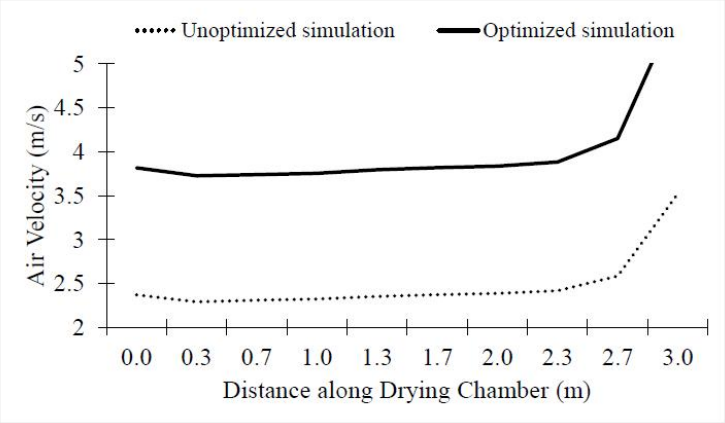

Fig. 25. Air velocity comparison before and after optimization along the drying chamber

Fig. 25 shows comparison of air velocity before and after optimization along the length of drying chamber.

It was observed from Fig. 25 that the velocity of the air within the drying chamber was slightly increased from 2.37 m/s to 3.82 m/s indicating an improvement of the drying rate [1]. Uniform velocity was noted throughout the drying chamber but there was a significant rise in velocity noted near the exhaust stack due to reduced flow cross section area.

4. CONCLUSION

It can be concluded from the study that Hybrid solar dryers have demonstrated success in drying almost all of the farm produce. Solar biomass hybrid dryers incorporate biomass stove- heat exchanger system to supplement solar radiation and allow continuous interrupted drying, hence improves the drying rate and preserves the quality of dried product [1]. Due to consistent airflow and Temperature distribution within the drying chamber, it can be reasoned that dried maize with uniform moisture content can be achieved with this dryer. Optimization results of the HSBD indicated that the air temperature within the drying chamber was increased from 46°C to 50°C and velocity from 2.37 m/s to 3.82 m/s.

COMPETING INTERESTS

Authors have declared that no competing interests exist.

REFERENCES

1. Aukah Jackis, Mutuku Muvengei, Nderitu Hiram, Onyango Calvin. Prediction of airflow and temperature distribution in

hybrid solar-biomass dryer using computational fluid dynamics. Journal of Sustainable Research in Engineering (JSRE). 2018;4(3):76-89.
2. Donkor Benjamin. Performance evaluation of a mixed mode solar dryer incorporating a backup heater for drying cocoyam slices. BSc. Thesis, Kwame Nkrumah University of Science and Technology, Kumasi; 2017.
3. International Business Machines, Corporation. Technical handbook of systems engineering; 1963.
4. FTF, Kenya fy 2011-2015 multi-year strategy. Feed the future. Tech. Rep., United States Government; 2011.
5. Tonui KS, Mutai EBK, Mutuli DA, Mbuge DO, Too KV. Design and evaluation of solar grain dryer with a back-up heater. Research Journal of Applied Sciences, Engineering and Technology. 2014;7(15):3036–3043.
6. Om Prakash, Anil Kumar. Historical review and recent trends in solar drying systems. International Journal of Green Energy. 2013;10:690–738.
7. Grain crop drying, handling and storage. Available:http://www.fao.org/3/i2433e/i2433e10
8. Emma C. Martina, James W. T. Yatesb, Kayode Ogungbenroa, Leon Aarons. Choosing an optimal input for an intravenous glucose tolerance test to aid parameter identification. Journal of Pharmacy and Pharmacology. 2017;69: 1275–1283.
9. ANSYS - CFX Solver Theory Guide.
10. Kiranoudis CT, Karathanos VT, Markatos NC. Computational fluid dynamics of industrial batch dryers of fruits. Drying Technology. 1999;17(1&2):1–25.
11. Ido Seginor, Dvora Kantz, Uri M. Peper, Nahum Levav. Transfer coefficients of several polythene green house cover. Journal od Agricultural Engineering Research. 1988;39(1):19–37.
12. Garg HP, Prakash J. Solar energy-fundamentals and applications. Tata McGraw-Hill Publishing Company Ltd.; 1997.
13. ANSYS Design Exploration User's Guide.
14. Kerich D, Aukah J, Ogola J. Development and evaluation of briquettes from rice husks and other agro-wastes. TUD Press, Verlag der Wissenschaften GmbH. 2013;Chapter 18:197–208. ISBN: 978- 3 - 944331-17-1.
15. Ajaykumar Menon. Structural optimization using ANSYS and regulated multiquadric response surface model. Msc. Thesis, University of Texas at Arlington; 2005.

© 2020 Aukah et al.; This is an Open Access article distributed under the terms of the Creative Commons Attribution License (http://creativecommons.org/licenses/by/4.0), which permits unrestricted use, distribution, and reproduction in any medium, provided the original work is properly cited.

Peer-review history:
The peer review history for this paper can be accessed here:
http://www.sdiarticle4.com/review-history/54074